FLIGHT PERFORMANCES ANALYSIS OF UAV MFD NIMBUS

Vasile PRISACARIU, Lucian SIMINONESCU

"Henri Coandă" Air Force Academy of Brașov, Romania
(aerosavelli73@yahoo.com, lucian.simi@yahoo.com)

DOI: 10.19062/2247-3173.2018.20.30

Abstract: *Low cost, fixed wing UAVs have become available for a series of missions aimed to acquire data and operation information at entry and middle level. The concepts of fixed wing mini-UAVs make a necessity for users to have a proper knowledge regarding the flight and operation performances, in order to select the best type of aircraft for the required mission.*

The article contains a series of flight performances analyses for MFD Nimbus including 2D airfoil and 3D wing analyses, but without considering aerodynamic interferences between wing-fuselage-tail.

Keywords: *aerodynamic analyzes, MFD Nimbus, FPV, XFLR5*

Symbols and acronyms

FPV	*First-Person Viewing*	*AoA*	*Angle of Attack*
VLM	*Vortex Lattice Method*	*AR*	*Aspect Ratio*
LLT	*Lifting Line Theory*	*MAC*	*Main Aerodynamic Chord*
V	*Air speed*	*GPL*	*General Public License*
TE / LE	*Trailing Edge / Leading Edge*	*BL*	*Boundary Layer*
GUI	*Graphical User Interface*	X_{CP}	*Pressure center position*
C_m	*Pitch moment coefficient*	*Re*	*Reynolds number*
C_L	*Lifting coefficient*	C_Y	*Lateral force coefficient*
C_D	*Drag coefficient*		

1. INTRODUCTION

Nimbus is an aircraft UAV manufactured by MFD (MyFlyDream). It features a V tail, two electrical engines on a rectangular wing. The front part of the fuselage is removable, thus allowing for the mounting of radio-electronic equipment, while the rear part of the body is made out of carbon. It is designed to be assembled and to be transported quickly, therefore all its body parts are made as simple as possible [1, 2].

FIG. 1 MyFlyDream Nimbus

Constructive features and radio-electronic equipment offer the capabilities of a UAV that can perform low-cost missions in the FPV concept used to acquire data in areas of interest in accordance with national law.

Table 1. Technical features, [1, 2]

Parameter	Value	Parameter	Value
Span / lenght	1800 mm / 1300 mm	Max. speed	130 km/h
Lift surface	37.5 dm^2	Endurance	1,5 .. 2,5 h
Max weight / Payload	5,5 kg / 1,5 kg	Max. ceiling	3500 m

The wide array of missions the Nimbus can perform are as follows: acquiring of data (both image and telemetric) which can be transmitted through the airborne radio equipment (GPS), of data regarding the atmosphere using its environmental sensors (temperature and humidity) and of data related to 3D behavior of the frame in its flight. The behavior of its structure is also recorded by mounted sensors (vibrations, twisting etc).

2. XFLR5 THEORETICAL GUIDELINES

XFLR5 is software featuring a wide range of geometrical modules (foil, wing, tail, fuselage, and aircraft) and of functions for aerodynamic computing (methods VLM, LLT and 3D panel) at GPL standards for the designing of sailplanes, a task for which the software will bear reasonable and consistent results.

Analysis algorithm used by XFLR5 it the same used by XFOIL and it makes possible a direct analysis using its own airfoils database. The airfoil is defined by: name, Reynolds and Mach numbers, transition point of turning from laminar to turbulent flow, upper and lower surfaces; figure 2, [3].

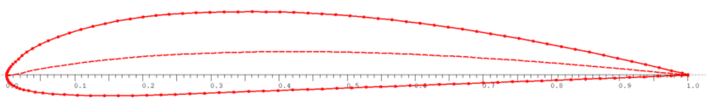

FIG. 2 Clark Y airfoil

2.1. 2D theoretical analysis

The 2D geometrical module contains functions for import/geometrical editing of a reliable airfoil and allows the user to configure the geometrical parameters of the foil such as: normalization; global and local refinement; editing the foil coordinates; camber and thickness of the airfoil the deflection of leading /trailing edge control surfaces fig. 3.

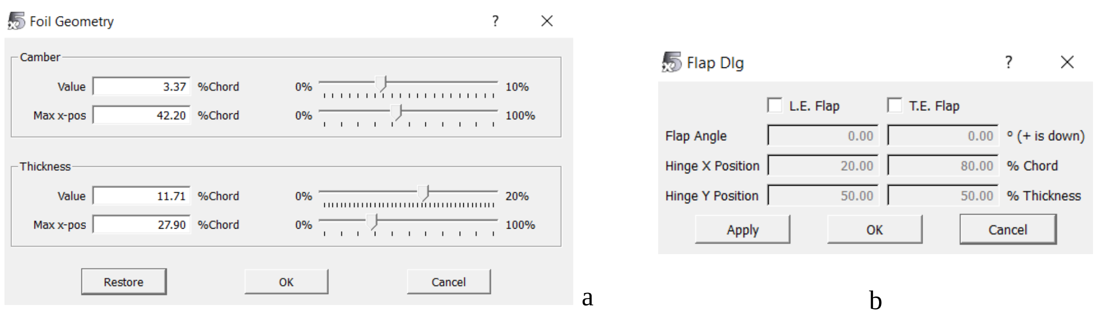

FIG. 3 2D geometric module XFLR5, a. chamber and thickness, b. flap [3]

A direct analysis of the airfoil contains: a numerical evaluation module for a specific Reynolds number, two series of numerical evaluation modules for an interval of Reynolds number values, one function to reset the computing data; an XFOIL module for the initial phase of the computing and a visualization function for the computational journal.

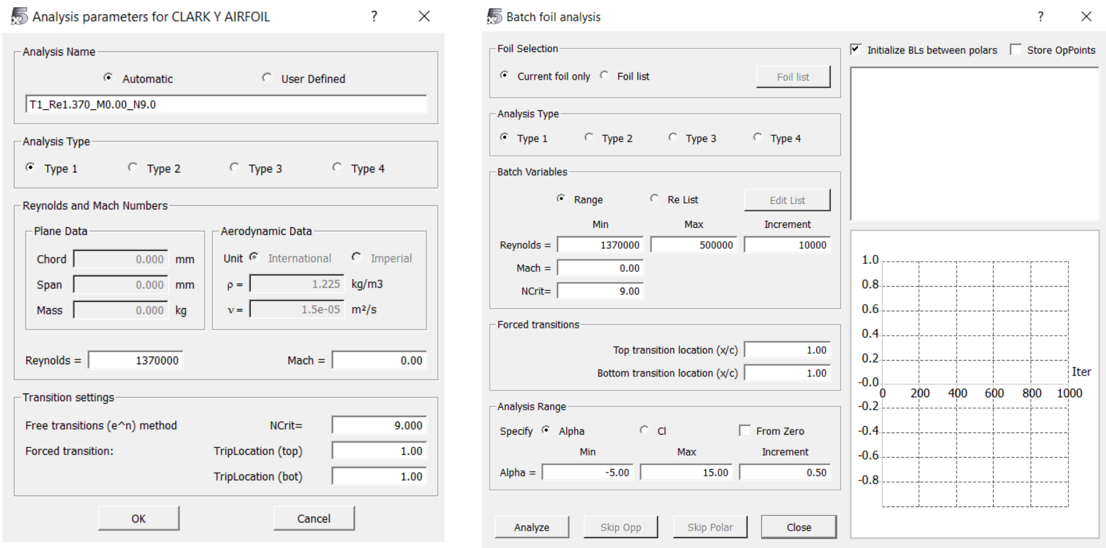

a b

FIG. 4 2D Direct analysis module for airfoil, a. Re numerical evaluation, b. interval Re numerical evaluation

After the setting of these initial conditions for analysis, the user can define the computing interval for the angle of attack, C_l or Reynolds number, resetting the option for the boundary layer (BL), viscous module and the OpPoint function which memorizes the analysis results. For the optimal viewing of the airfoil polars, the user can define a color and thickness for the curves resulted from the numerical simulation as well as displaying the initial conditions for the airfoil, Fig. 5.

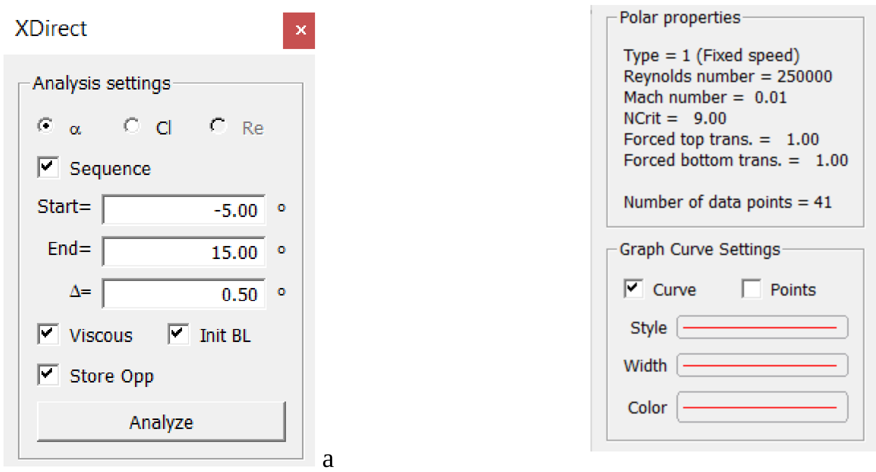

a b

FIG. 5 Initial settings of the direct numerical analysis,
a. AoA range, b. display of the initial conditions and visual polar settings

2.2. 3D theoretical analysis

For the geometric configuration of the wing, the user has available a geometric module which can be used to set the chord values; chords coordinates (axis O_x and O_y/offset); dihedral; wing washout; airfoil; type and number of computing panels on O_x and O_y axis; fig. 6.

For a guided user interface (GUI), the geometric module has a display for numerical geometric data for the defined wing; display options on all three axis, isometric; scaling of the wing and the save option for the defined model; fig. 6.

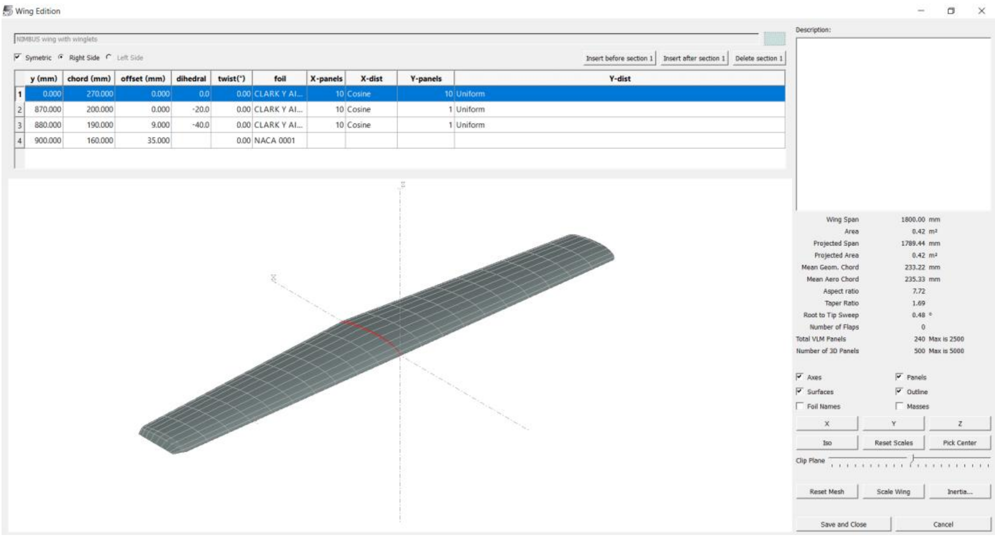

FIG 6 3D geometric module of the singular wing

The 3D analysis of the wing includes a sub-module for the aerodynamic analysis and one for stability analysis. The aerodynamic analysis used in this article is initialized by a series of computing parameters such as: air velocity, polar type, inertial properties, analytical method (LLT, VLM, and 3D panels); viscous/non-viscous module; figure 7.

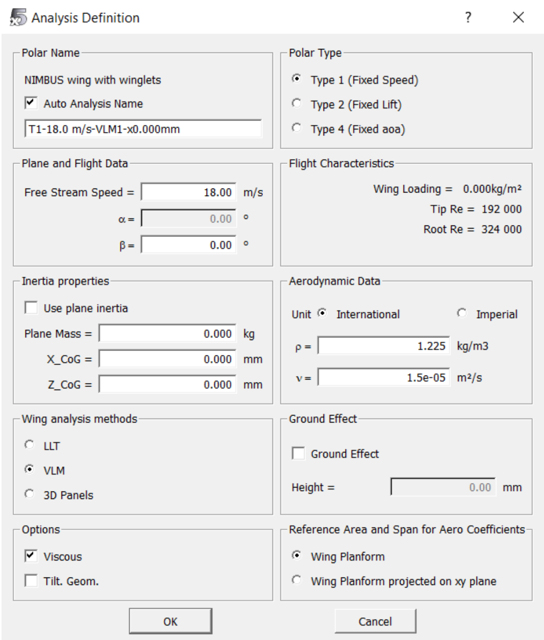

FIG. 7 Numeric analysis module

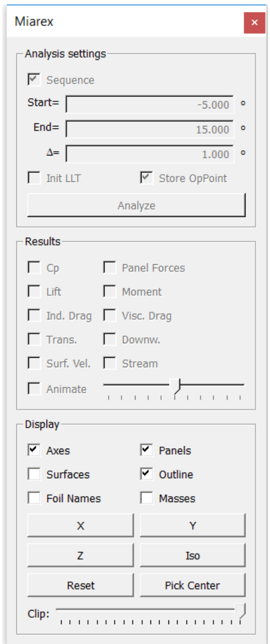

FIG. 8 Analysis functions and view of results

GUI offers displaying functions for the analyzed geometry and for the results: C_l, induced drag, pitching moment (C_m), vortices; figure 8.

3. AERODYNAMIC ANALYZES

For the aerodynamic analyses was used XFLR 5 [3, 4, 5, 12] which offers the instruments needed for the 2D/3D geometry and 3 methods of analyses: VLM, LLT, 3D panel method. For this article we have chosen bi-dimensional aerodynamic analyses for the airfoil and 3D analyses for the wing in 2 specific configurations.

3.1.2D airfoil analysis

The analysis conditions respect the actual speed range (65 ÷ 130 km / h) and the range of AoA for Nimbus MFDs flight, see Table 3.

Table 3. Analysis conditions, [2, 3]

Parameter	Value	Parameter	Value
Re	$2{,}5 \times 10^5 \div 5 \times 10^5$	Air kinematic viscosity	$1{,}42 \times 10^{-5}$
Iterations	1000	AoA	$-5^0 \div 15^0$
Airfoil	Clark Y		

The stages of the 2D airfoil analysis includes: the choosing of the foil geometry (Clark Y) designed in 1922, used for powered and unpowered aircraft, [7, 8, and 9]; the refinement stage of the global foil geometry (maybe redefining the number of characteristic points), the foil analysis stage (defining the Reynolds number interval and the angle of attack interval).

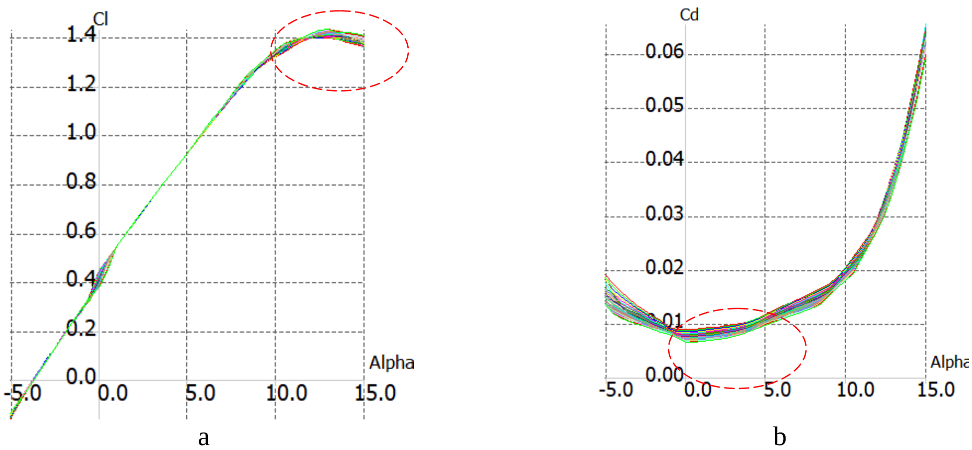

FIG. 2 The polars – aerodynamics coefficient, a. C_l-AoA, b. C_d-AoA

The value of the maximum lift coefficient be seen in figure 2a corresponding to the angle of attack of 12^0, and the drag coefficient increases exponentially after an angle of attack exceeding 10^o (figure 2b).

The pitching moment coefficient (C_m) shows a constant growing instability in the interval AoA=$1^o \div 14^o$ (figure 3a). The analyses airfoil has a maximum C_l to C_d ratio around of AoA=4^o (figure 3b). For a highly reliable aerodynamic analysis with a higher level of accuracy, the usage of mathematical computing software like Matlab, Maple, is required [10, 11].

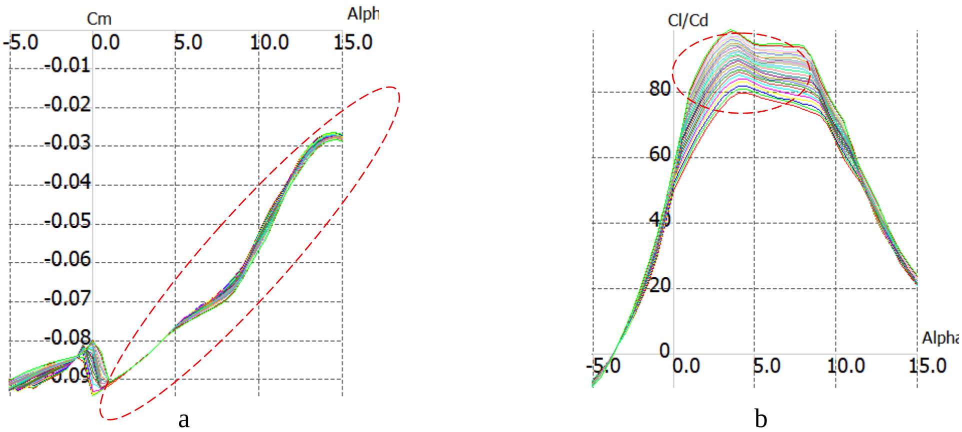

FIG. 3 The polars – aerodynamics coefficient, a. C_m vs. AoA, b. gliding ratio C_l/C_d vs. AoA

3.2. 3D wing analysis

The 3D geometry analysis requires the usage of 1:1 scale for the Nimbus wing; see figure 4 and table 4.

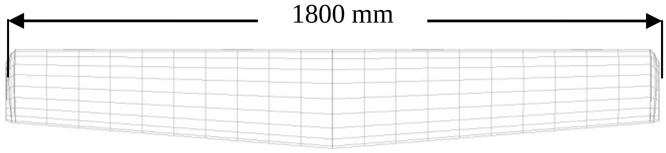

FIG. 4 MFD Nimbus wing

The geometric configuration of the wing analysis presents a mesh made up of 10 panels for wing span and 10 panels for chord.

Table 4. Geometric features, [2, 3]

Parameters	Value	Parameter	Value
Airfoil	Clark Y	Surface	0,42 m^2
Span	1800 mm	Twist	0^0
C_0 / C_e	270 mm / 200 mm	AR	7,72
Taper ratio	1,69	MAC	235 mm

The initial conditions for the analysis highlight the real flight limitations of MFD Nimbus; see table 5.

Table 5. Initial conditions, [2, 3]

Parameter	Value	Parameter	Value
Re	$2{,}5 \times 10^5 \div 5 \times 10^5$	Air kinematic viscosity	$1{,}42 \times 10^{-5}$
Iterations	100	AoA	$-5^0 \div 15^0$
Method	LLT / VLM	Tip Re / Root Re	192000 / 324000
Polar	Constant speed	Speed	18 m/s
Boundary conditions	Dirichlet	VLM/ 3D panels	240 / 500
Angle sideslip	0^o		

The 3D aerodynamic analysis of the wing generates the variation of the main aerodynamic characteristics (figure 5 and 6) using 2 analysis methods (LLT and VLM). The computing situation is made at the characteristic minimum speed of 18 m/s.

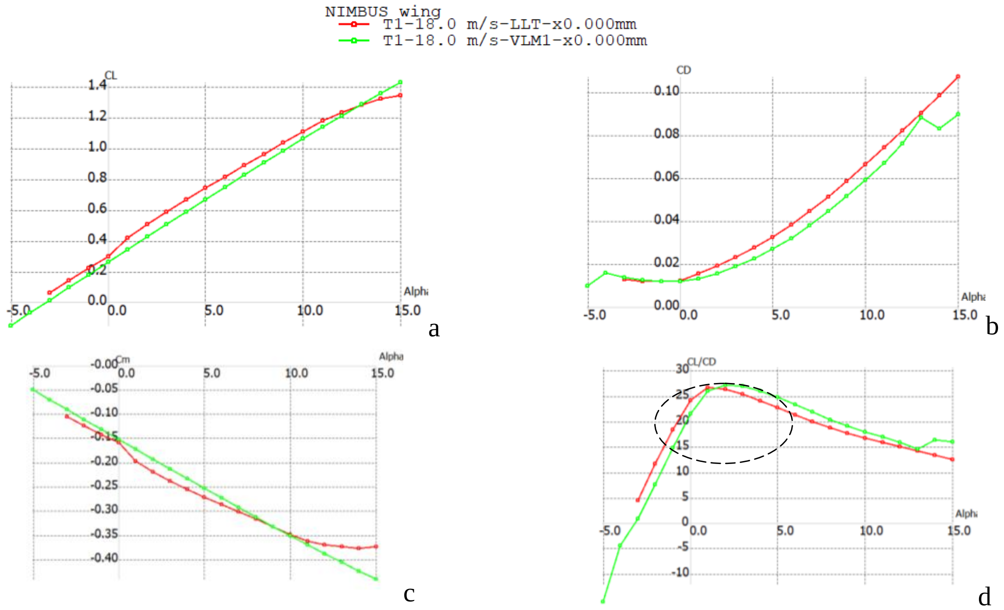

FIG. 5 Aerodynamic features of the singular wing for MFD Nimbus at V=18 m/s, a. C_L vs. AoA, b. C_D vs. AoA, c. C_m vs. AoA, d. gliding ratio C_L/C_D vs. AoA

LLT and VLM methods have produced close results for the C_l on the interval $1^o \div 9^o$ (figure 5a) while the C_d rises exponentially in a similar manner after AoA=5^0 (figure 5b). The slope of the pitching moment coefficient keeps a constant value and the actual value of the C_m has close values for the both types of analysis (figure 5c). The maximum gliding ratio (C_L/C_D vs. AoA) has a maximum value at AoA=$2 \div 3^o$, with small absolute differences (-0,23 vs. -0,27), figure 5d.

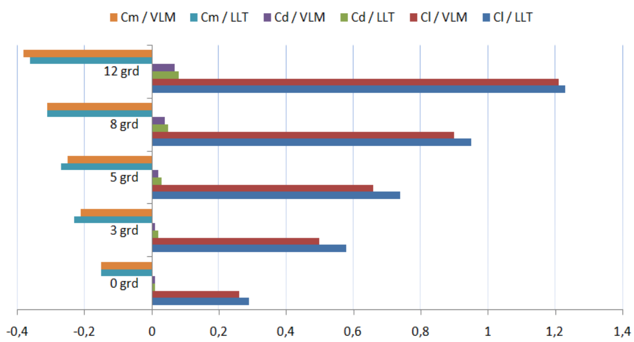

FIG. 6 Comparative charts with date for 18 m/s

Fig.7 highlights the lift distribution on the wing and the drag for each wing segment with the changes in angle of attack. With an increasing air velocity, the analysis shows a corresponding increase in drag at the wing tips.

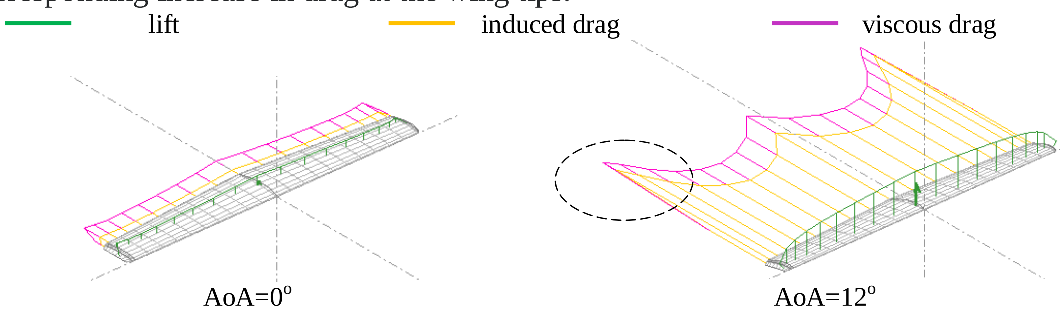

FIG. 7 The variation of lift and drag function of the angle of incidence (AoA) for V=18 m/s

4. CONCLUSIONS

The article drew the guidelines of a preliminary aerodynamic analysis for a classical configuration of an operational UAV (MFD Nimbus). This analysis was center on the 2D airfoil and the 3D wing geometry.

The analysis of an airfoil in viscous conditions using XFOIL offer good, efficient and precise results, but it also has its errors (the compressibility corrections are invalid) when the airfoil has an irregular geometry of its leading edge or has one which is too sharp (invalid geometrical settings).

XFLR5 is a freeware (GPL) instrument which can be successfully used for estimations of the aerodynamic performances of: unpowered, fixed-wing aircraft (estimated values with aerodynamic interferences), lifting singular surfaces (wings, tails), bodies of revolutions (fuselages, fairings) and other aerodynamic bodies (various fairing, floats).

In order to achieve highly reliable results the user needs precise geometric features for the working models and also very well defined analysis settings and restrictions.

ACKNOWLEDGMENT

The National Authority for Scientific Research, Romania supported this work – CNCS-UEFISCDI: with PN-III-P2-2.1-PED-20161972, MAPIAM project, contract 65PED/2017.

REFERENCES

[1] MFD Nimbus, available at https://www.fpvmodel.com/myflydream-mfd-nimbus-1800-long-range-rc-fpv-plane-kit-only_g1273.html , accessed at 12.03.2018;

[2] MFD Nimbus, available at http://www.myflydream.com/index.php?main_page=product_info&products_id=28&cPath=1&language=en, accessed at 12.03.2018;

[3] Drela M., Yungren H., *Guidelines for XFLR5 v6.03 (Analysis of foils and wings operating at low Reynolds numbers)*, 2011, available at http://sourceforge.net/projects/xflr5/files, accessed at 12.03.2018;

[4] Prisacariu V., Cîrciu I., Boşcoianu M., *Flying wing aerodynamic analysis*, REVIEW OF THE AIR FORCE ACADEMY, 2/2012, Braşov, Romania, ISSN 1842-9238; e-ISSN 2069-4733, p 31-35;

[5] Prisacariu V, Boşcoianu M, Cîrciu I., *Management of robotic aerial systems accomplishment* , RECENT Journal 2/2012, Transilvania University of Brasov, Romania, ISSN 1582-0246, p. 203-217;

[6] *Airfoil tools*, available at http://airfoiltools.com/airfoil/details?airfoil=clarky-il, accessed at 14.03.2018,

[7] *Airfoil design*, 18p., available at www.mail.tku.edu.tw/095980/airfoil%20design.pdf, accessed at 19.03.2018;

[8] Selig D., Selig F., *Airfoil at low speed*, publisher H.A. Stokely, USA, 1989, 408p, available at www.m-selig.ae.illinois.edu/uiuc_lsat/Airfoils-at-Low-Speeds.pdf;

[9] Lyin C.A., Broeren A.P. and other, *Summary of Low-Speed Airfoil Data*, SoarTech Publications, ISBN 0-9646747-3-4, 1997, 454p., http://m-selig.ae.illinois.edu/uiuc_lsat/Low-Speed-Airfoil-Data-V3.pdf;

[10] Rotaru C., Cîrciu I., Boscoianu M., *Computational methods for the aerodynamic design*, Review of the Air Force Academy, 2(17)/2010, ISSN:1842-9238, p43-49;

[11] Anderson, Jr., John, D., *Fundamentals of Aerodynamics*, Fourth Edition, McGraw Hill, New York, USA, 2007;

[12] Vural M., *Estimating R/C model aerodynamics and performance*, p. 1-13, available at https://mypages.iit.edu/~vural/RC%20Airplane%20Design.pdf.